Artifacts and landmarks: pearls and pitfalls for in vivo reflectance confocal microscopy of the skin using the tissue-coupled device

Melissa Gill[1,2], Christi Alessi-Fox[3], Kivanc Kose[4]

Affiliations: [1]SkinMedical Research and Diagnostics, P.L.L.C, Dobbs Ferry, New York, USA, [2]Department of Pathology, SUNY Downstate Medical Center, Brooklyn, New York, USA, [3]Caliber Imaging & Diagnostics, Inc, Rochester, New York, USA, [4]Dermatology Service, Memorial Sloan-Kettering Cancer Center, New York, New York, USA

Corresponding Author: Melissa Gill, SkinMedical Research and Diagnostics, P.L.L.C, P.O. Box 42, Dobbs Ferry, NY, USA & Department of Pathology, SUNY Downstate Medical Center, Brooklyn, NY, Tel: 914-478-0549, Email: MGill@SkinMedicalRandDx.com

Abstract

Reflectance confocal microscopy (RCM) is a non-invasive imaging tool for cellular-level examination of skin lesions, typically from the epidermis to the superficial dermis. Clinical studies show RCM imaging is highly sensitive and specific in the diagnosis of skin diseases. RCM is disseminating from academic tertiary care centers with early adopter "experts" into diverse clinical settings, with image acquisition performed by technicians and image interpretation by physicians. In the hands of trained users, RCM serves an aid to accurately diagnose and monitor skin tumors and inflammatory processes. However, exogenous and endogenous artifacts introduced during imaging can obscure RCM images, limiting or prohibiting interpretation. Herein we review the types of artifacts that may occur and techniques for mitigating them during image acquisition, to assist technicians with qualitative image assessment and provide physicians guidance on identifying artifacts that may confound interpretation. Finally, we discuss normal skin "landmarks" and how they can *(i)* obscure images, *(ii)* be exploited for additional diagnostic information, and *(iii)* simulate pathological structures. A deeper understanding of the principles and methods behind RCM imaging and the varying appearance of normal skin structures in the acquired images aids technicians in capturing higher quality image sets and enables physicians to increase interpretation accuracy.

Keywords: reflectance confocal microscopy, basal cell carcinoma, melanoma, malignant melanoma, in vivo imaging, skin cancer, dermatology, nevus, nevi, melanocytic, mimickers, artifacts, actinic keratosis, fungus, pitfalls, best practices, image acquisition, mosaic, mosaicking

Introduction

Reflectance confocal microscopy (RCM) is a non-invasive imaging tool that allows for in vivo evaluation of skin at the cellular level. In the hands of trained users, RCM can be used as an aid to accurately diagnose and monitor several types of tumors and inflammatory processes in vivo [1-14]. However, exogenous and endogenous artifacts can obscure RCM images, limiting or prohibiting interpretation. Exogenous artifacts are related to the optical, mechanical properties of RCM, or the device handling by the operator leading to problems at the skin-microscope interface. Generally, these artifacts can be avoided through user training on RCM functions and proper RCM setup for imaging. Endogenous artifacts are patient- or lesion-related and in general harder to avoid. A solid foundation in the RCM features of normal skin and its structures is crucial for both imaging technician and reader not only to fluently navigate the images, but also to avoid diagnostic pitfalls. The aims of this article are: 1) to characterize the types of artifacts that can occur during image acquisition using the tissue-coupled RCM, identify their causes, describe their effect on

Abbreviations:

AIC	Automatic Intensity Correction
BCC	Basal Cell Carcinoma
DEJ	Dermal-Epidermal Junction
FOV	Field of View
MC	Meissner Corpuscles
RCM	Reflectance Confocal Microscopy
TCRCM	Tissue Coupled Reflectance Confocal Microcopy

image interpretation and how they can be prevented, and 2) to describe how skin landmarks can obscure images, aid diagnosis, and mimic pathological structures.

Mechanics of RCM: A basic understanding of the principles and methods behind RCM is essential to comprehend how artifacts are created and mitigated. RCM captures images ("optical sections") with quasi-histologic resolution in the horizontal (en face) plane at user-selected depths from the surface of the epidermis to the superficial dermis. These optical sections are achieved by two systems within the device: illumination and detection. The illumination system includes a near-infrared 830nm diode laser, an array of lenses, and scanning optics that focus emitted light into a volume (voxel) in the tissue, where it is scattered by natural tissue components (proteins and pigments). The detection system uses the same optics to collect the back-scattered reflection and focus it on a photo-detector to record its intensity. The microscope scans tissue voxel-by-voxel in a raster fashion (spatial resolution 0.5-1µm) to obtain an image of the in-focus en face section of skin. A pinhole located on the detection path rejects back-scattered light from out-of-focus structures, resulting in en face "optical sections" with 3-5µm axial resolution. RCM images are gray-scale because the illumination is a single wavelength. The refractive index difference between structures results in a change in back-scattered light providing contrast [15-17]. Keratin, melanin, and melanosomes are highly scattering (reflecting), appearing white. Organelles in leukocytes are moderately scattering, appearing light grey. Nuclei and plasma mostly absorb light, appearing dark grey to black (15, 16, 18, 19]. In addition to these, both endogenous and exogenous structures (e.g. air bubbles trapped in imaging oil, hair, ducts, and Meissner corpuscles) also scatter light [15, 16].

The tissue-coupled RCM (TCRCM), VivaScope 1500 Caliber Imaging & Diagnostics, Inc, Rochester, NY, attaches to the skin via medical adhesive on an imaging window, which stabilizes the device relative to the tissue. Mineral oil (index fluid) is required between the window and the tissue surface and ultrasound gel (immersion fluid) is required between the objective lens and the window in order to minimize optical aberrations by matching the refractive indices at these contact surfaces. The TCRCM offers single image, stack, mosaic, and video capture [17]. A stack corresponds to a series of single field-of-view (0.5×0.5mm) en face images at a fixed spatial location collected at consecutive depths (with fixed intervals). Mosaicking involves moving the imaging window together with the skin coupled beneath it relative to the objective lens and collecting multiple single field-of-view images at neighboring spatial locations at a fixed focusing depth. The collected images are then stitched together to form a larger field-of-view en face mosaic image. Capturing up to 8×8mm mosaics is possible using the current commercially available device [17, 18]. TCRCM is also equipped with a dermoscopic camera. Prior to coupling the RCM, one should capture a dermoscopic image. As the camera and the RCM use the same imaging window, their fields of view are spatially registered, allowing the technician to use the dermoscopic image as a map to precisely navigate the RCM within the lesion [19].

Discussion

In the following sections, we will describe and illustrate artifacts that are frequently encountered during RCM imaging. Artifacts are grouped into two main categories *(i)* exogenous and *(ii)* endogenous artifacts. Readers should keep in mind that these two groups are not independent and various combinations of these artifacts may take place in a single mosaic or RCM image depending on the circumstances.

Data presented in this paper were retrieved from an archive of images collected under IRB approved protocols. Prior to RCM imaging, all study subjects signed an informed consent to an institutional review board approved protocol of either *(i)* a multi-center study at University of Rochester, Loma Linda University Medical Center, Skin and Cancer Associates, and Memorial Sloan Kettering Cancer Center or *(ii)* a study at University of Modena and Reggio Emilia. All studies and the experiments were conducted in accordance with Declaration of Helsinki principles.

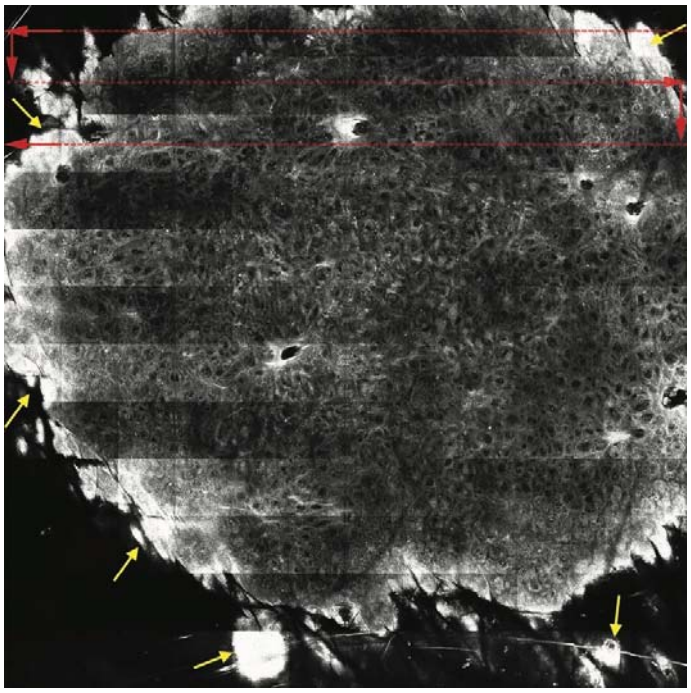

Figure 1. *Illumination and AIC artifacts - saturated areas and striping 6×6mm mosaic of a papule showing (i) saturated tissue edges where there is a transition from black index fluid filled voids to tissue (yellow arrows) and (ii) "striping" or alternating bands of bright and dark images illustrating the time lapsing as AIC adjusts.*

Exogenous artifacts

Illumination artifacts are one of the most encountered artifacts in RCM imaging. Saturated (too bright) or under-illuminated (too dark) areas within images occur when the reflective properties of the imaged area change rapidly. The microscope adjusts the laser power intensity to maintain the mean signal as the imaging location changes (spatial or axial motion). This functionality is called automatic intensity control (AIC). This adaptation is intentionally kept gradual to avoid flickering in image brightness. Therefore, AIC cannot always compensate for abrupt changes in intensity between consecutive imaging locations, resulting in some images that are saturated or under-illuminated. For example, in RCM mosaics, sharp transitions can be encountered around large wrinkles, large follicles, or at the edges of concavities/papules. The voids of wrinkles, hair follicles, concavities, and imaged area surrounding papules typically appear dark on RCM as they are oil-filled (**Figures 1-3**), [20-22]. The AIC function automatically increases laser power, aiming to increase average signal level. Unfortunately, such areas are also typically surrounded by stratum corneum, which is highly reflective (appears bright/white) owing to its keratin content [20, 21] and would require a more rapid reduction in laser power than AIC allows to avoid becoming saturated (**Figures 1, 2**).

The AIC adjustment results in horizontal stripes of alternating bright and dark bands throughout the mosaic. The "striping" artifact (**Figure 1**) is most pronounced in superficial mosaics and becomes less problematic in deeper mosaics. The coordination of image capture, AIC, and mosaicking is critical in producing high quality images. Therefore, AIC is factory-configured and cannot be adjusted by the user. The effect can be eliminated by temporarily

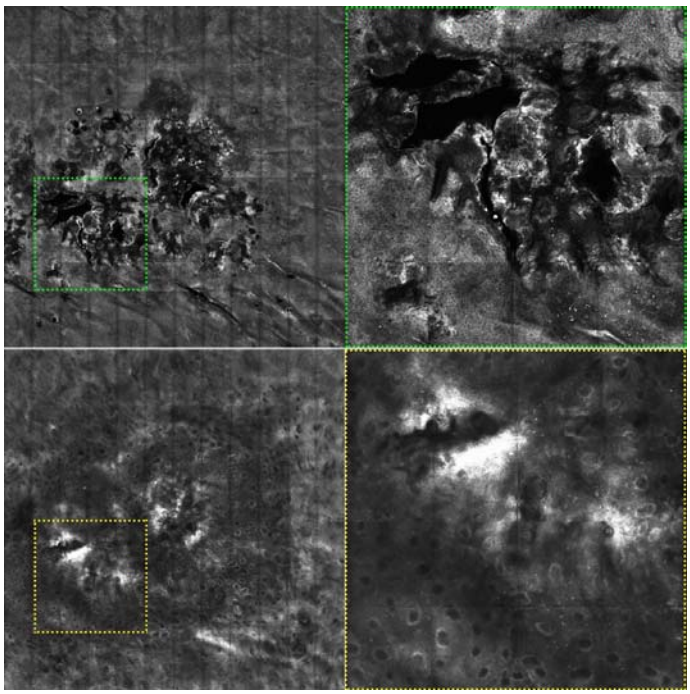

Figure 2. *Crusted, hyperkeratotic, papillated lesion with concave center and shower-glass effect. 6×6mm superficial (top left) mosaic shows black, oil-filled crevasses of a centrally concave lesion. Upper panel inset (green box) shows a 2×2mm submosaic of at the level of stratum spinosum (rimmed by bright stratum spinosum) in papillated areas surrounding the black concavities, where the tissue surface has yet to be reached. Lower panel shows a deeper 6×6mm mosaic and 2×2mm submosaic inset (yellow box) where the majority of the lesion is at the DEJ level, but the base of the concavity is bright, hyper-reflective stratum corneum. This deeper mosaic also illustrates the shower-glass effect, where foci appear dark with loss of resolution due to excessive scattering of light through overlying crusts/hyperkeratosis. The mosaic grid pattern is visible in the larger mosaics.*

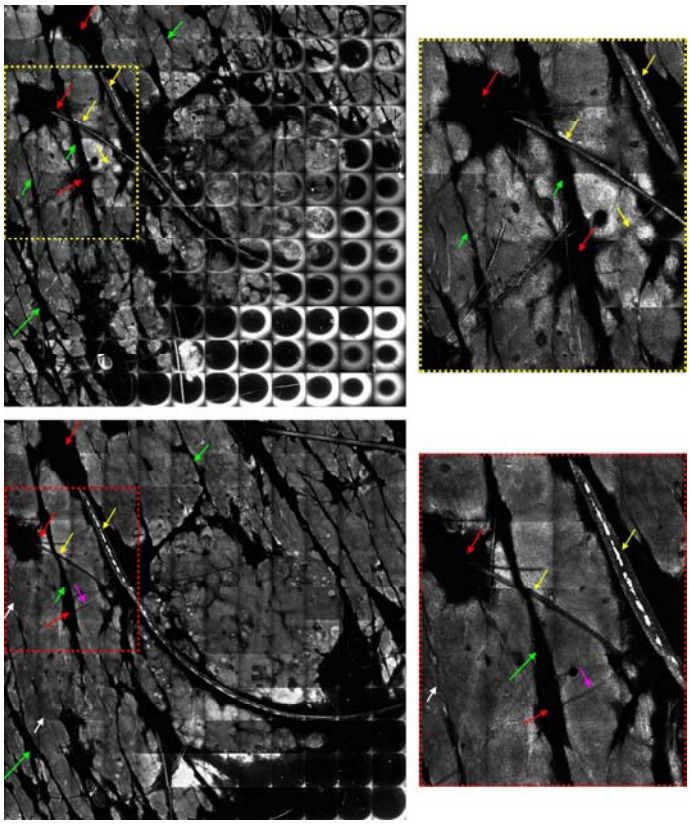

Figure 3. *Skin folds, hair follicles and hair shafts. 6×6mm mosaics and insets (2×3mm) showing dark oil-filled "valleys" of skin folds (green arrows) and follicular orifices (red arrows) from which hair shafts of varying caliber protrude (yellow arrows). In the deeper mosaics (bottom row), one can see the linear dark "shadows" (magenta arrow) with loss of resolution created by the overlying reflective hair shaft and the white lines representing the base of the skin fold "valleys," as the reflective stratum corneum is imaged (white arrows). This figure also illustrates the mosaic grid pattern and tangential imaging, where a wide range of tissue levels are present in a single mosaic. The circular pattern due to surface reflections from the imaging window is noted in the bottom right corner of the upper left mosaic and the images become progressively deeper toward the top left corner, where stratum granulosum/stratum spinosum is seen (yellow inset).*

turning off the AIC function in the software and manually adjusting the laser power between each mosaic before initiating capture. This, however, requires the technician to adjust the laser power between each mosaic and can still result in under-illuminated or saturated images if the adjustment is not made in an optimal location as there is no ability to adjust the power during mosaic capture. In new systems (4th generation), AIC automatically sets the laser power to the appropriate intensity prior to each mosaic capture and maintains its state without adjustment during acquisition to eliminate the striping effect. Similarly, during stack imaging, the time and AIC adjustment between each image capture is optimized to eliminate flicker, saturation, under-illumination, or partial illumination. Stacks are automatically configured to capture images at a pace that reduces motion artifacts, but sometimes AIC is slower to adjust, which can result in darker images deeper in the dermis. For most clinical applications, the loss of intensity in the deeper stack images does not prohibit interpretation.

Loss of resolution occurs with increasing imaging depth. This is an optical limitation of RCM imaging rather than an artifact. Skin is a turbid volume, whose imaging properties change as a function of depth. Through this turbid volume, the resolution of imaging depends on *(i)* how refractive and scattering properties change and *(ii)* how much laser power can be delivered as a function of depth. The former *(i)* is the real source of resolution loss, as the focused laser beam disperses and lose its coherence as it travels deeper into the skin leading to optical distortions related to tissue heterogeneity. As a result, in vivo RCM images deeper than 150-200µm typically lack diagnostic quality.

Mosaic grid pattern results from natural vignetting that leads to illumination reduction at the edges of the images. For practical design purposes (reducing size and cost), RCM objective lenses do not have a flat field-of-view (FOV), which means light reflecting from the points at the border of the FOV comes back

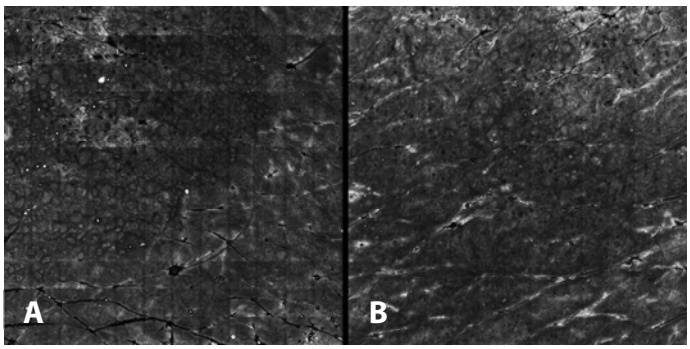

Figure 4. *Mosaic grid pattern.* ***A)*** *The mosaic on the left captured with the 3^{rd} generation microscope shows grid pattern overlaying the image. On the contrary, in the mosaic on the right* ***B)****, which was collected using the 4^{th} generation microscope, the grid pattern is virtually imperceptible. Both mosaics cover 6x6 mm field of view.*

to the imaging sensor at an angle, resulting in less signal intensity. The edges of each RCM image therefore often appear darker, resulting in a dark grid-like pattern highlighting the edges of individual RCM images tiling the mosaics **Figure 4**). In the research setting, it is possible to correct this artifact by applying the inverse of the illumination profile by post-processing the mosaics. In 4th generation of the microscope, modifications to the optics allow for mosaicking in vertical strips (strip mosaicking), eliminating the horizontal seams. By appropriately calibrating the FOV, allowing for overlap of the strips and aligning them, the vertical grid lines are virtually eliminated, providing near-seamless mosaics.

Oblique images may occur while imaging contoured, rigid surfaces, such as forehead or scapula. In this scenario, the imaging window applies variable pressure to the imaged area, compressing part of the skin more than others. This results in oblique mosaics, where one side is deeper than the other and multiple anatomic levels of the skin are captured in the same mosaic (**Figure 3**). This artifact can be minimized by positioning the patient so that the site of interest is perpendicular to the device and the tissue window has maximum contact, minimizing stress on the adhesive. Moreover, one must be sure that the tissue window is seated properly in the tissue cone-attachment without any tilt. As this artifact is directly proportional to the spatial distance traversed by the microscope during imaging, one can also minimize it by limiting the mosaic area and collecting multiple adjacent mosaics rather than one large mosaic on bony contoured sites such as zygoma.

Detachment of the imaging window may take place during leveling and positioning the TCRCM if *(i)* excessive stress is introduced on the adhesive or *(ii)* oil is smeared over the surface preventing the imaging window to securely adhere to the skin. If maximum contact is not achieved, the additional stress introduced by the motion of the microscope during mosaicking may result in detachment. To avoid such problems, a drop of oil can be placed on the window and carefully distributed with the tip of the applicator rather than applying the oil directly to the skin, which risks contaminating the adhesive. If

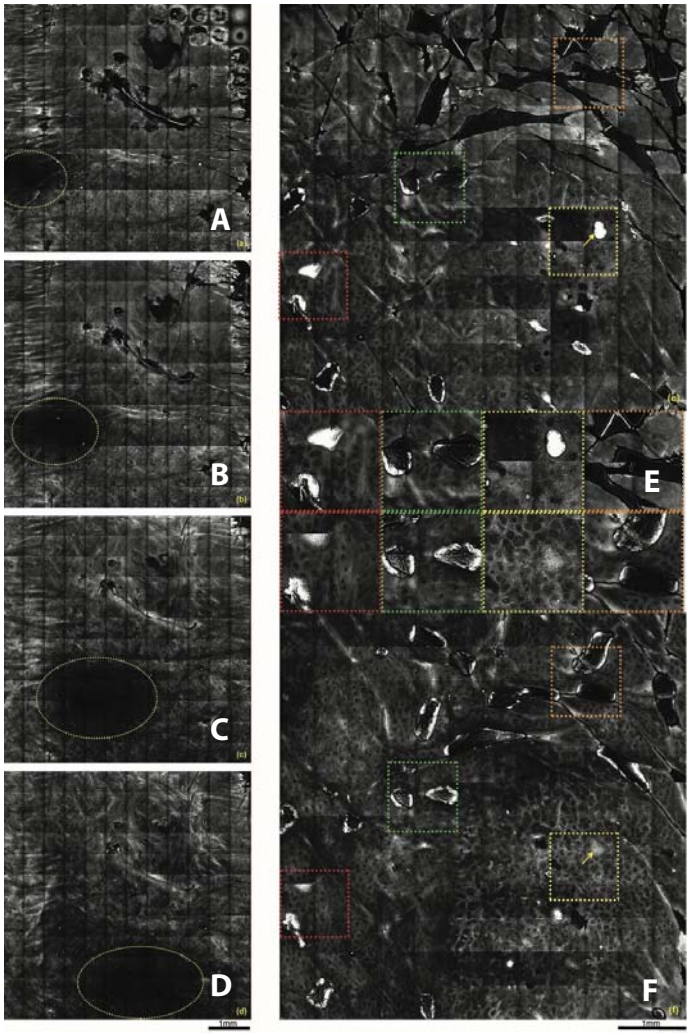

Figure 5. *Air bubbles trapped in gel/oil **A-D)** (Left), 6×6mm mosaics at subsequent depths show a dark shadow (yellow dashed oval) created by a bubble in the gel (immersion fluid) traveling horizontally across the mosaics and ultimately spreading over a larger area as the objective lens moves within the gel. **E, F)** (Right), 6×6mm mosaics at subsequent depths plus 1×1mm insets show the varying morphologies of air bubbles trapped in oil (index fluid) and how they change with increasing imaging depth. The red insets show irregular round to indented bright structures superficially, which become more fringed on the deeper mosaic. The green inset shows similarly shaped bubbles also filling surface irregularities or adnexal ostia, but rather than being bright, these thinner bubbles show a bright periphery and an internal fringe pattern with similar brightness to the surrounding tissue. The bubble (yellow arrow) in the yellow insets, fills a round indent, probably an eccrine ostium, and is bright white, mimicking a milial cyst, but the fringe pattern on the deeper mosaic, which could be confused with a melanocytic nest, confirms that this is a bubble. The orange inset shows thin bubbles filling the wrinkles. On the deeper mosaic, these appear similar to the bubbles in the green insets. Of note, all of these images also display some degree of the mosaic grid pattern.*

the window detaches during positioning or imaging, the mosaics will be unregistered with the dermoscopic image and may miss the targeted area. If window detachment occurs, the skin should be thoroughly cleaned with alcohol, a new imaging window should be applied, and the entire imaging procedure should be restarted.

Air bubbles trapped in ultrasound gel (immersion fluid) or mineral oil (index fluid) often create artifacts in RCM images. The refractive index of air (n= 1) is lower than fluid or tissue (N=1.3-1.5) leading to undesired refraction of the light passing through the interface.

Air bubbles trapped in ultrasound gel (immersion fluid) cast a shadow in the underlying image. This shadow typically moves around the image owing to the motion of the objective lens within the gel during mosaic capture (**Figure 5A-D**). If the bubble is small (100-200µm), it is often pushed outside of the imaged field and the shadow disappears. When large (>200µm), however, a significant part of the mosaic appears dark. When this occurs, the gel can be wiped

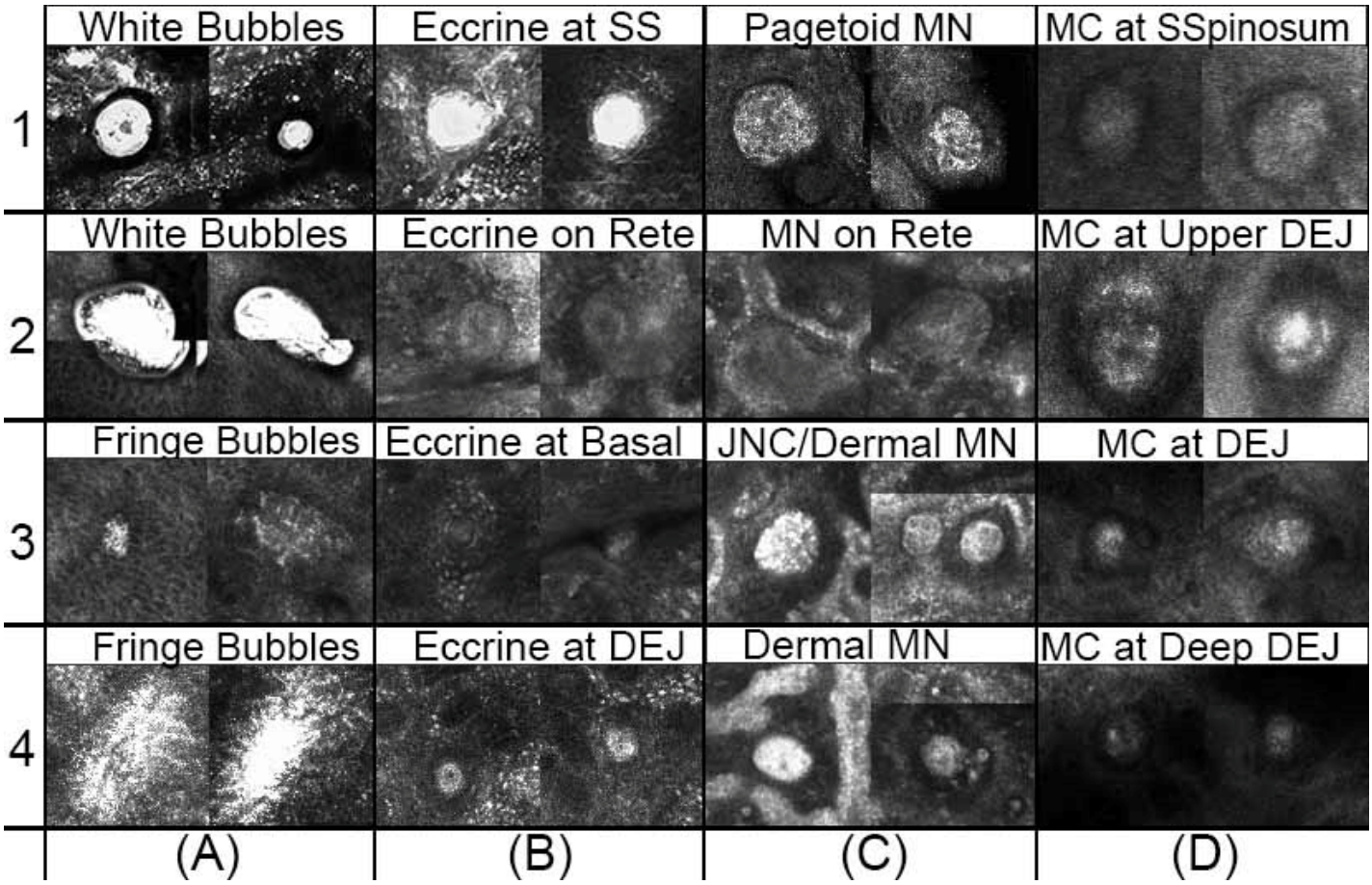

Figure 6. *Mimickers. This series of images (0.2×0.2mm - 100×100 pixels) demonstrates how similar various structures can appear when viewed in isolation, confirming the importance of context when interpreting RCM images. Column A shows the differing appearances of air bubbles trapped in oil from the skin surface to the DEJ (Frames A1-A4). The presence of air bubbles is confirmed by reviewing images captured at the surface of the skin. Column B shows the differing appearances eccrine ducts from stratum spinosum (SS) to within dermal papillae at the dermal-epidermal junction (DEJ). The presence of eccrine ducts is confirmed by identifying the characteristic "coil" of a duct through the epidermis. Eccrine ducts can range from donut-shaped to very bright round structures to darker homogeneous grey round structures. Column C illustrates the appearance of intraepidermal melanocytic nests (MN), (C1), junctional (JNC) MN (C2, C3) and dermal MN (C3, C4). Column D shows the different presentations of Meissner's corpuscles (MC), which while always at the tips of dermal papillae may appear to be intraepidermal (D1) in certain locations. Nests on acral surfaces are ruled out by the clinical context and recognizing the patterned location of MC. Eccrine ducts are ruled out by following the structure through the epidermis to confirm the presence or absence of the characteristic "coil" of a duct.*

out of the window and replaced without replacing the imaging window. Bubbles in gel are reduced by not shaking the bottle of gel and storing it cap-side down.

Air bubbles trapped in oil (index fluid) can be introduced by shaking the oil prior to use or, applying oil to wet skin (leftover alcohol or water after cleaning). In addition, the presence of excessive scale or hair can make it difficult for oil to penetrate all cracks/crevices. Air bubbles trapped in oil are typically round or polymorphous (depending on location) and brighter than or, if thin, of similar intensity to surrounding tissue (**Figure 5E, F)**. Bubbles trapped in adnexal ostia often show a bright appearance visible in each mosaic and may mimic keratin-filled milia/pseudocysts and, on superficial acral skin, eccrine ducts (See also Landmarks section, **Figure 6**). Thin air bubbles trapped on the skin's surface show a fringe pattern in deeper mosaics, which can mimic a cellular nest (See also Landmarks section, **Figure 6**). Toggling between superficial and deep images usually enables distinction between bubbles and their mimics (**Figure 5E, F)**. Air bubbles in oil are reduced by *(i)* not shaking the index oil, *(ii)* shaving hairy skin, *(iii)* thoroughly cleaning the skin using an alcohol prep pad, *(iv)* allowing skin to dry completely, and *(v)* uniformly distributing oil to the window before applying the window to the skin.

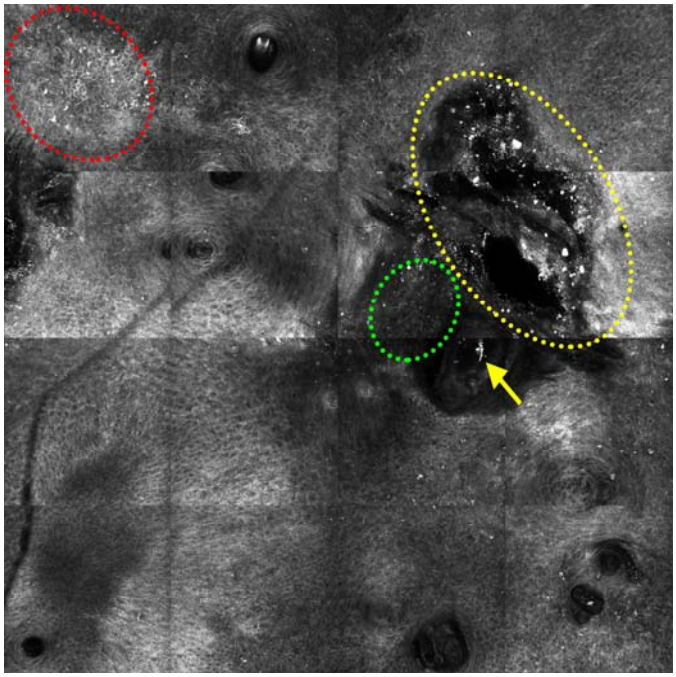

Figure 7. *Particulates. Numerous variably-sized white particular and short filamentous structures are present within a complex follicular rostium (yellow oval and arrow). Notice how the particulates can be similar in size and shape to pagetoid cells and dendrites (red oval). This image also shows how the valleys of ostia can be used to identify parakeratosis (green oval). A mosaic grid pattern is visible.*

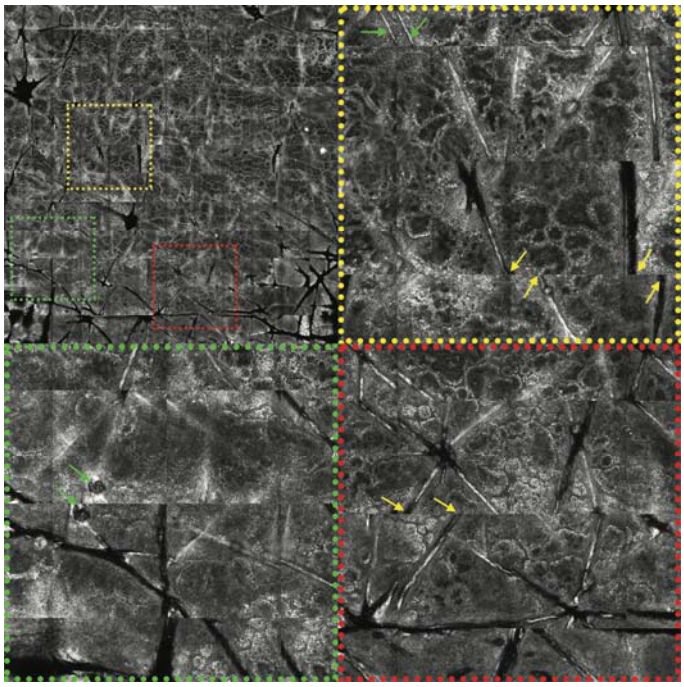

Figure 8. *Stitching artifact. 5.75×5.75mm mosaic and 1.5×1.5mm submosaic insets show artifacts created by shifting of individual images resulting in mosaics with features that are repeated (green arrows) or not aligned vertically along stitch-points (yellow arrows).*

Particulates on the skin from cosmetics or sunscreens reflect light owing to their high refractive index (n>1.5). They appear on the skin surface as large or small bright particles (**Figure 7**). Regular application of these products accumulates in hair follicles and in some deep wrinkles. Therefore, small residual particles may still be visualized even after thorough cleaning with soap and water followed by an alcohol prep pad prior to imaging. Although not usually a confounder, these particles may occasionally mimic melanin or pagetoid cells in the superficial epidermis.

Endogenous artifacts

Patient motion artifacts occur when the skin moves in the axial or lateral plane relative to the device during image and mosaic capture and include misaligned

stacks, stacks with images out of order, and mosaic stitching artifacts. Axial motion appears as images captured out of order in stacks or images jumping back and forth between skin layers in mosaics and stacks. It is usually seen on the chest or back caused by talking or, breathing and movements related to heartbeat or pulse points (e.g. temporal artery) caused by arterial flow. Lateral motion leads to misalignment of a stack or shift/non-matching borders between adjacent images in a mosaic (**Figure 8**) and is typically caused by moving and talking, but significant loss of tissue elasticity related to actinic damage can also cause this defect. Motion can be minimized by allowing the patient to lie fully supported on an examination table, using pillows or bolsters to further support imaging the extremities and asking the patient to remain still and not speak for the duration of image capture. The patient can be asked to hold their breath during stack capture, if tolerable.

Blurry images with early loss of resolution can be seen in lesions that are hyperkeratotic, have high melanin content (abundant and/or larger intraepidermal melanin granules), or both. These conditions can be encountered in skin conditions such as certain squamous neoplasms, hyperkeratotic dermatitides, heavily pigmented melanocytic neoplasms or keratoses, and lesions on patients with Fitzpatrick skin phototypes V and VI [15, 16, 20, 21, 23-25]. Excessive scattering of light reflecting from keratin and/or melanin causes a blurring effect of some structures (**Figure 9**) and prevents light from penetrating deeper levels of the tissue resulting in premature loss of resolution. Novice readers may not recognize this and over-call benign structures. For example, edged papillae that are blurry may be misinterpreted as non-edged. If hyperkeratosis prevents visualization of the dermal-epidermal junction (DEJ) and/or dermis, one can gently pare down the stratum corneum with a scalpel blade prior to imaging. Nonetheless, one must proceed with caution understanding that hyperkeratosis and/or hypermelanosis may limit interpretation and biopsy may be needed [23-26].

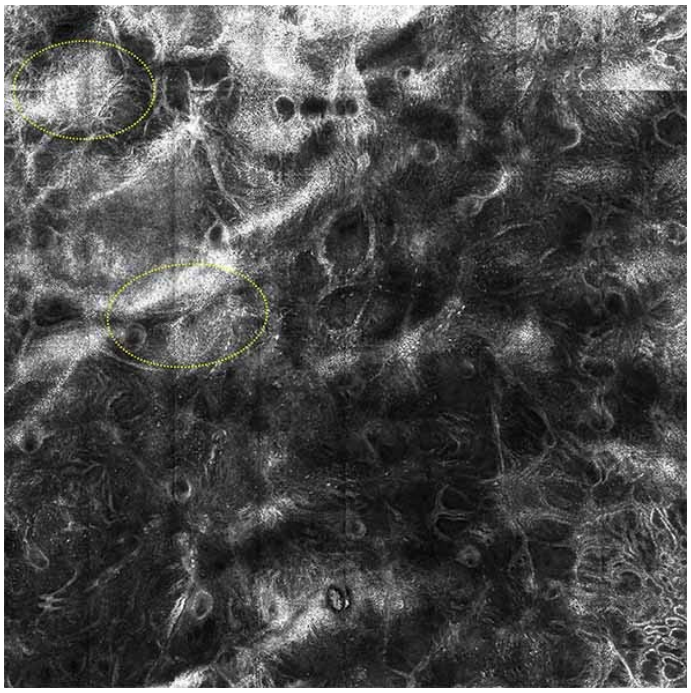

Figure 9. *Blur caused by hyperpigmentation. In this 4×4mm mosaic of a melanocytic neoplasm, heavily pigmented areas disperse a disproportionate amount of light causing these foci to be saturated and blurry (yellow ovals).*

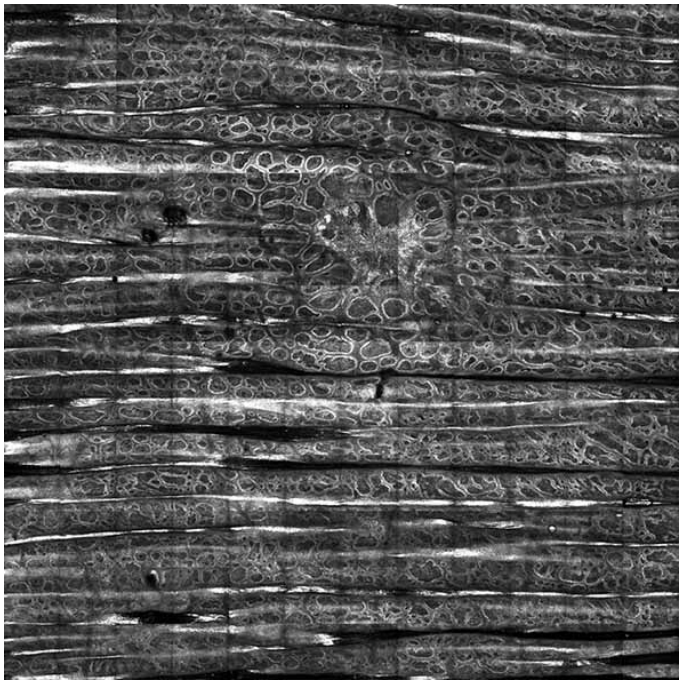

Figure 10. *Wrinkles due to advanced age. Multiple horizontal parallel fine wrinkles typical of skin on an elderly patient with significant actinic damage can be seen in this 6×6mm mosaic. Note, the wrinkles appear dark when imaging the oiled-filled valley and bright when the stratum corneum at the base of the wrinkle is reached. The mosaic grid pattern is also visible.*

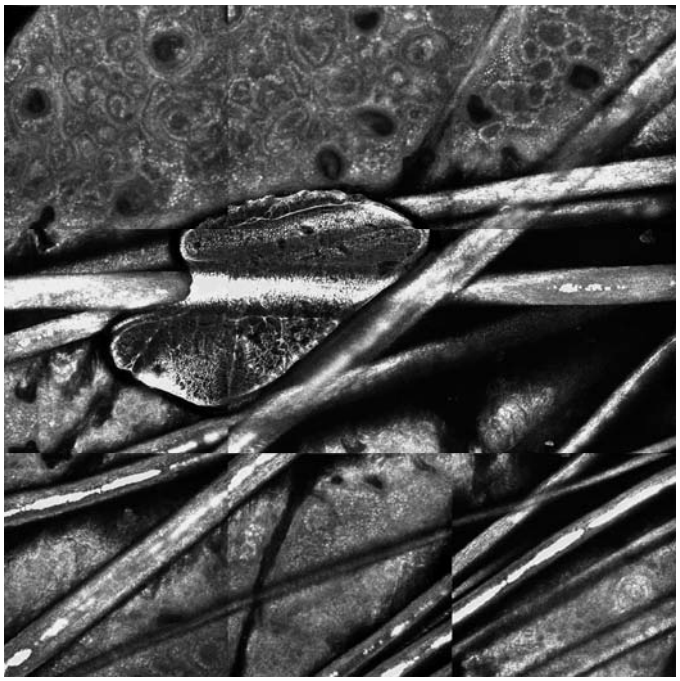

Figure 11. *Numerous hair shafts entrapping bubble. This 1.5×1.5mm submosaic illustrates how numerous hair shafts can trap air bubbles in the oil and how the combination of numerous hair shafts and bubble obscure a large portion of the image, rendering it non-diagnostic. In this situation, shaving prior to imaging is necessary to obtain quality images.*

Interestingly, the homogeneous, tightly packed, specialized corneocytes of acral skin harbor low scattering properties, allowing light to penetrate non-lesional skin several hundred microns without introducing blur. However, the stratum granulosum on these surfaces tends to be highly scattering. Furthermore, on pressure points such as the bottom of the first toe, the acral epidermis is so thick that the maximal working distance of the objective lens (~400µm) is often reached prior to the DEJ. However, RCM reliably reaches the upper dermal papillae on non-lesional non-weight-bearing acral skin, such as fingertip, thenar eminence, or foot arch, allowing for non-invasive examination of Meissner corpuscles in peripheral neuropathy [27-30].

Shower-glass effect occurs when imaging through heterogeneous crusts. Crusts are comprised of varying combinations of serum, inflammatory cells, bacteria, fibrin, and erythrocytes, and can be present over ulcerated or non-ulcerated skin. Thin crusts are often fairly homogeneous and weakly scattering. If a crust is thick and contains several structures, such as inflammatory cells, which reflect a lot of light, images will appear blurry and lose resolution early, similar to excessively keratotic or melanized lesions. Many crusts are heterogeneous in shape, composition, and thickness, causing uneven light penetration creating a "shower glass effect", with islands showing better resolution (under low scattering crust) speckled between blurry areas with poor resolution (under high scattering crust), (**Figure 2**). When imaging crusted lesions, if the crust's diameter measures less than 4mm, the ring can be centered on the crust, but image quality during capture should be assessed in non-crusted tissue to ensure an adequate number of mosaics are captured at all epidermal levels and superficial dermis. If the crust is greater than 4mm in diameter, the ring should be centered on the most clinically suspicious non-crusted portion of the lesion. Any diagnosis should be made with caution in crusted lesions and biopsy must be considered before rendering a benign diagnosis [23, 25].

Dark images superficially occur in a few different settings, such as eroded lesions with minimal crusting, concave lesions, and papules. Eroded lesions may appear dark superficially when the stratum corneum and stratum granulosum are missing, as the spinosum is normally not very reflective. During imaging, only elevated areas, such as the periphery of concave lesions (**Figure 2**) and the center of papules (Figure1), that are in contact with the window will be visible initially. The less elevated portions will appear dark as the image captured is within the oil-filled "void." If the elevation difference is not greater than the maximum working distance of the objective lens, deeper images should capture the non-elevated tissue without loss of resolution usually associated with that working distance. In lesions with vastly uneven surfaces, more than one set of images may be required to ensure representative sampling.

Landmarks: helpful tips and pitfalls to avoid

Skin folds (furrows) or wrinkles are "valleys" in the skin surface. In RCM images, they appear as dark, linear structures that narrow in deeper successive images [21, 22, 31]. The side walls of "valleys," formed by the stratum corneum, are typically perpendicular or oblique to the imaging plane (**Figure 3**). Hence, as one moves away from the dark line of the skin fold,

the level quickly transitions first from bright stratum corneum, to stratum granulosum, followed by stratum spinosum in vertical or transverse planes until meeting the horizontal plane made up by the majority of the image. Sometimes, the stratum corneum of a skin fold, follicular orifice, or other surface invagination is the easiest place to identify diagnostic features such as parakeratosis (**Figure 7**) or fungal hyphae [5]. Furthermore, if melanocytes are seen next to the dark line of a skin fold, they may represent pagetoid cells and be helpful to support a melanoma diagnosis [13, 32, 33]. Immediately below the dark line formed by a skin fold, one finds a white line indicating that stratum corneum is reached at the base of the valley (**Figure 3**). Here, the layers of the skin are viewed in the horizontal plane but will again be discordant with those of the majority of the RCM image allowing for another opportunity to look for diagnostic features of more superficial levels. In patients with extensive loss of elasticity and thinning of the skin (usually related to aging and actinic damage) one can see many thin, closely spaced, adjacent wrinkles throughout the entire imaged field (**Figure 10**).

Hair shafts appear on RCM as a bright linear structure emanating from dark roundish areas, which are the follicular orifices (**Figure 3**). Owing to high keratin and varying melanin content, hair has a highly reflective nature, which interferes with the passage of light, degrading the subjacent image quality and creating a linear dark "shadow" (**Figure 3**). However, unlike a wrinkle, the dark line is at the same anatomic level as surrounding skin. Air bubbles can also become trapped in the oil between the hair shafts (**Figure 11**). In areas of very dense hair (e.g. scalp, chest of some men), shaving prior to imaging reduces this artifact. However, the effect is minimal with vellus or rare terminal hairs and not shaving

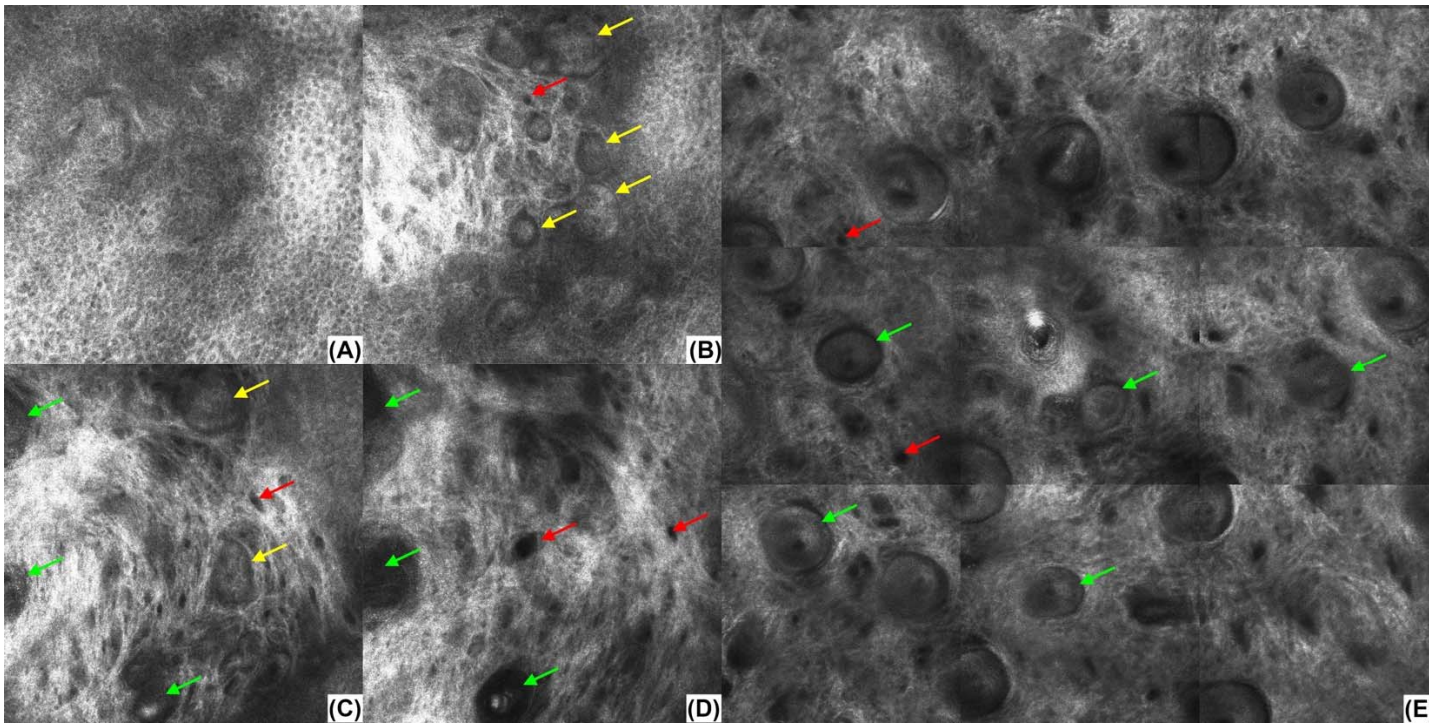

Figure 12. *BCC mimicking vellus follicle.* ***A-D)*** *(0.75×0.75mm) are successively deeper images captured with a handheld RCM. At the surface of the skin* ***(A)****, there is cellular atypia but an absence of follicular openings, confirming the absence of vellus hairs in the imaged field. Images* ***(B)*** *and* ***(C)*** *show small BCC tumor nests (yellow arrows) with peripheral palisading and peritumoral dark cleft-like spaces at the base of epidermis and in the papillary dermis. Within the deeper dermis* ***(D)****, the superficial tumors are no longer visible; however, hair follicles (green arrows) first seen in subtly in* ***(C)*** *enter the field of view more clearly in* ***(D)****. Small blood vessels (red arrows) are also visible in the dermis* ***(B-D)****.* ***E)*** *(1.50×1.50mm mosaic) normal facial skin shows multiple vellus hair follicles with palisading and clefting (green arrows), typically observed in en face images in addition to small blood vessels (red arrows).*

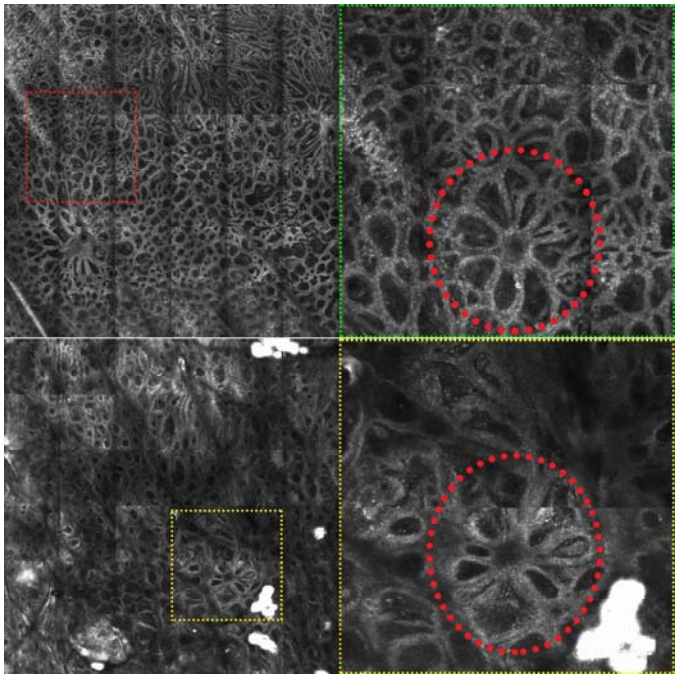

Figure 13. *Eccrine flowers. In these 3×3mm submosaics with 1.5×1.5mm submosaic insets of melanocytic neoplasms, eccrine ducts can quickly be identified by the characteristic daisy flower pattern (circled in insets) created by a central eccrine duct with radiating rete enclosing papillary dermis to create the petals. The mosaic grid pattern is most prominent in the upper left image and bright white bubbles (air trapped in oil) are noted in the lower image and bottom left of the yellow inset.*

may be advantageous as sparse hairs can serve as landmarks to allow for direct correlation with other imaging modalities [20, 27].

Hair follicles (**Figure 3**) provide unique landmarks for image comparisons but can also be a pitfall for diagnosis. When comparing dermoscopy, RCM, and histopathology to further understand how various structures appear across viewing platforms, hair follicles, like hair shafts, can help navigate and confirm location. The varying appearances of hair follicles on RCM [20, 27] are also important to recognize as certain diagnoses characteristically feature follicular involvement, such as lentigo maligna, lupus, and lichen plano-pilaris [2, 9, 14], whereas a lack of follicular involvement can help in differentiating actinic keratosis from squamous cell carcinoma in situ on RCM mosaic images [34]. Moreover, it is important to avoid the pitfall of mistaking a vellus hair follicle, which also can show peripheral palisading and a dark cleft-like rim, from basal cell carcinoma (BCC), (**Figure 12**), [23, 27]. This is particularly difficult when no hair shaft is protruding, which can often happen on the head and neck. In this situation, one should follow the structure to the surface in more superficial mosaics or stacks and look for concentric follicular epithelial layers surrounding a central orifice. Of less importance, dermal portions of hair follicles can also be confused with eccrine ducts, a problem which can also be solved by following the structure superficially [27]. Rarely, a novice reader may confuse a dilated follicular orifice, which lacks a hair shaft, with a dermal papilla. Again, this error is avoided by following the structure in more superficial or deeper levels.

Eccrine ducts, present in varying numbers across the entire skin surface, can also be a cause of diagnostic confusion for the less experienced RCM reader. Recognition of the repetitive location of eccrine ducts (which varies from frequent and aligned on palms and soles to more sparse on abdomen), the eccrine ductal coiling down from the epidermal surface into the dermis, the subtle "donut-like" morphology in more superficial mosaics or stacks, and the daisy pattern at the DEJ created by radially oriented rete rimming petal-shaped papillary dermal islands around central eccrine ducts (**Figure 13**) aids in correctly identifying eccrine ducts [20, 22, 27]. Eccrine ducts at the level of DEJ or dermis may appear as a bright round structure and be misinterpreted as a melanocytic nest (**Figure 13**). Owing to loss of resolution with increasing imaging depth, eccrine ducts can also resemble a dense homogenous round nest at the tip of a rete ridge (**Figure 6**). In the dermis, it can also be challenging to distinguish eccrine ducts from vellus hair follicles and small BCC nests [23], (**Figure 6**).

Meissner corpuscles (MC) are site specific normal skin structures that can represent a diagnostic pitfall [27]. Meissner corpuscles, specialized mechanoreceptors involved in touch pressure sensation, are located in the tips of dermal papillae of fingertips, palms, soles, genitalia, lips, and eyelids. On RCM, they appear as heterogeneously bright roundish structures within dermal papillae. On sites such as the arch of the foot, where epidermal architecture shows relative acanthosis with papillae extending high up into the

epidermis, Meissner corpuscles located just below the suprapapillary plate are seen in intraepidermal mosaic layers otherwise showing granular or spinous keratinocytes and giving the false impression that they are located within the epidermis. As a result, the novice reader may misinterpret these MCs as pagetoid nests or eccrine ducts (**Figure 6**). In healthy individuals, MCs are regular in size and regularly distributed, creating a pattern which serves as a clue to their true nature. However, in areas with prior trauma or in patients with peripheral neuropathy, such as diabetic neuropathy or chemotherapy-induced neuropathy, MCs can vary in size and be irregularly distributed, increasing the likelihood of misinterpretation, which is especially problematic when evaluating a melanocytic proliferation at the level of the granular layer as small nests at this location would be concerning for malignancy [27-30].

Conclusion

Adopting new technology, such as TCRCM, requires training in the principles and methods as well as a fluent knowledge of the myriad presentations of normal skin to avoid pitfalls. Many artifacts encountered during in vivo imaging of the skin are avoidable if one understands how they are created. Recognizing the limitations of RCM and artifact effects on imaging allows the technician to collect a complete high-quality image set and the physician to identify non-representative sampling. Furthermore, it enables the RCM reader to separate diagnostic features from artifacts. Being aware of how artifacts and normal structures can mimic each other as well as pathological structures is the key in minimizing avoidable diagnostic errors. As RCM disseminates from the hands of experts and is adopted more widely, the nuanced detail of the practice must be passed to ensure quality care.

Potential conflicts of interest

Melissa Gill is a paid research consultant on investigator-initiated grant funded by DVB Technologies, and Christi Alessi Fox is a shareholder and employee of Caliber I.D. Inc, the manufacturer of the VivaScope. Kivanc Kose declares no conflict of interest.

References

1. Nori S, Rius-Díaz F, Cuevas J, et al. Sensitivity and Specificity of Reflectance-Mode Confocal Microscopy for in Vivo Diagnosis of Basal Cell Carcinoma: A Multicenter Study. *J Acad Dermatol.* 2004;51: 923–30. [PMID: 15583584].
2. Ardigo M, Longo C, Gonzalez S. Multicentre Study on Inflammatory Skin Diseases from the International Confocal Working Group: Specific Confocal Microscopy Features and an Algorithmic Method of Diagnosis. *Br J Dermatol.* 2016;175: 364–74. [PMID: 26948927].
3. Hofmann-Wellenhof R, Pellacani G, Malvehy J, Hans Soyer PH. editors. In: *Reflectance Confocal Microscopy for Skin Diseases*. Springer Berlin Heidelberg; 2010. [DOI:10.1007/978-3-642-21997-9].
4. Tan M. J, Lambie D, Sinnya S, et al. Histopathology and Reflectance Confocal Microscopy Features of Photodamaged Skin and Actinic Keratosis. *J Eur Acad Dermatol Venerol.* 2016;30: 1901–11. [PMID: 27298142]
5. Friedman D, Friedman CP, Gill M. Reflectance Confocal Microscopy: An Effective Diagnostic Tool for Dermatophytic Infections. *Cutis* 2015; 95: 93–97. [PMID: 25750962].
6. Ayelet R, Kim N, Scope A, et al. Reflectance Confocal Microscopy Criteria for Squamous Cell Carcinomas and Actinic Keratoses. *Arch Dermatol* 2009;145: 766–72. [PMID: 19620557].
7. Carrera C, Ulrich M. Nonmelanocytic Tumors In S. González (Ed.) Reflectance Confocal Microscopy of Cutaneous Tumors. CRC Press; 2017. [DOI: 10.1201/9781315113722].
8. Longo, C. Melanocytic Tumors. In S. González (Ed.) Reflectance Confocal Microscopy of Cutaneous Tumors. CRC Press; 2017. [DOI: 10.1201/9781315113722].
9. Ardigò, M, Agozzino M, Franceschini C, et al. Reflectance Confocal Microscopy for Scarring and Non-Scarring Alopecia Real-Time Assessment. *Arch Dermatol Res* 2016;308: 309–18. [PMID: 27225248].
10. Gill M, González S. Enlightening the Pink: Use of Confocal Microscopy in Pink Lesions. *Dermatol Clin* 2016;34: 443–58. [PMID: 27692450].
11. Pellacani G, Farnetani F, González S, et al. In Vivo Confocal Microscopy for Detection and Grading of Dysplastic Nevi: A Pilot Study.*J Acad Dermatol* 2012;66: e109–e121. [PMID: 21742408].
12. Guitera P, Scolyer AR, Gill M, et al. Reflectance Confocal Microscopy for Diagnosis of Mammary and Extramammary Paget's Disease. *J Euro Acad Dermatol.* 2013;27: e24–e29. [PMID: 22211938].
13. Pellacani G, Guitera P, Longo C, et al. The Impact of in Vivo Reflectance Confocal Microscopy for the Diagnostic Accuracy of Melanoma and Equivocal Melanocytic Lesions. *J Invest Dermatol.* 2007;127: 2759–65. [PMID: 17657243].
14. Pascale G, Pellacani G, Crotty AK, et al. The Impact of in Vivo Reflectance Confocal Microscopy on the Diagnostic Accuracy of Lentigo Maligna and Equivocal Pigmented and Nonpigmented Macules of the Face. *J Invest Dermatol.* 2010;130: 2080–91. [PMID: 20393481].

15. Rajadhyaksha, M, Grossman M, Esterowitz D, Webb HR, Anderson RR. In Vivo Confocal Scanning Laser Microscopy of Human Skin: Melanin Provides Strong Contrast. *J Invest Dermatol.* 1995;104: 946–52. [PMID: 7769264].
16. Rajadhyaksha, M, González S, Zavislan JM, Anderson RR, Webb HR. In Vivo Confocal Scanning Laser Microscopy of Human Skin II: Advances in Instrumentation and Comparison with Histology. *J Invest Dermatol.* 1999;113: 293–303. [PMID: 10469324].
17. Larson B, Rajadhyaksha M, Abeytunge S. Fundamentals of Reflectance Confocal Microscopy In S. González (Ed.) Reflectance Confocal Microscopy of Cutaneous Tumors. CRC Press; 2017. [DOI: 10.1201/9781315113722].
18. Que SKT, Fraga-Braghiroli N, Grant-Kels JM, et al. Through the Looking Glass: Basics and Principles of Reflectance Confocal Microscopy. *J Acad Dermatol.* 2015;73: 276–84. [PMID: 26051696].
19. Que SKT, Grant-Kels JM, Rabinovitz HS, Oliviero M, Scope A. Application of Handheld Confocal Microscopy for Skin Cancer Diagnosis: Advantages and Limitations Compared with the Wide-Probe Confocal. *Dermatol Clin*. 2016;34: 469–75. [PMID: 27692452].
20. Leib JA, Gill M, Patel YG, Rajadhyaksha M, González S. Normal Skin In Reflectance Confocal Microscopy of Cutaneous Tumors: An Atlas with Clinical, Dermoscopic and Histological Correlations. Halpern A, (Ed.), Informa UK Ltd; 2008. [DOI: 10.3109/9780203091562].
21. Ardigo M, Gill M, Floristan U, et al. Normal skin: Terminology In S. González (Ed.) Reflectance Confocal Microscopy of Cutaneous Tumors. CRC Press; 2017. [DOI: 10.1201/9781315113722].
22. Cinotti E, Perrot JL. Topographic and Skin Phototype Variations of Skin with Special Emphasis on Facial and Acral Skin In S. González (Ed.) Reflectance Confocal Microscopy of Cutaneous Tumors. CRC Press; 2017. [DOI: 10.1201/9781315113722].
23. Gill M, Jain M, Alessi-Fox C, González S. Reflectance Confocal Microscopy – Histology Correlations for Nonmelanocytic Tumors In S. González (Ed.) Reflectance Confocal Microscopy of Cutaneous Tumors. CRC Press; 2017. [DOI: 10.1201/9781315113722].
24. Ulrich M, Zalaudek I, Welzel J. Shining into the White: The Spectrum of Epithelial Tumors from Actinic Keratosis to Squamous Cell Carcinoma. *Dermatol Clin.* 2016;34: 459–67. [PMID: 27692451].
25. Longo C, Farnetani F, Ciardo S, et al. Is Confocal Microscopy a Valuable Tool in Diagnosing Nodular Lesions? A Study of 140 Cases. *Br J Dermatol* 2013;169: 58–67. [PMID: 23374159].
26. Ulrich M, Oliviero M, Rabinovitz HS. Squamous Neoplasia (subtypes) and Progression In S. González (Ed.) Reflectance Confocal Microscopy of Cutaneous Tumors. CRC Press; 2017. [DOI: 10.1201/9781315113722].
27. Gill M, Jain M, Gamo R, González S, Alessi-Fox C. Adnexal and Sensory Structures of the Skin In S. González (Ed.) Reflectance Confocal Microscopy of Cutaneous Tumors. CRC Press; 2017. [DOI: 10.1201/9781315113722].
28. Herrmann DN, Boger NJ, Jansen C, Alessi-Fox C. In Vivo Confocal Microscopy of Meissner Corpuscles as a Measure of Sensory Neuropathy. *Neurology*. 2007;69: 2121–7. [PMID: 17898322].
29. Almodovar JL. Ferguson M, McDermott MP, et al. In Vivo Confocal Microscopy of Meissner Corpuscles as a Novel Sensory Measure in Cmt1a. *J Peripher Nerv Sys.* 2011;16: 169–74. [PMID: 22003930].
30. Almodovar JL, Schifitto G, McDermott PM, Ferguson M, Herrmann DN. HIV Neuropathy: An in Vivo Confocal Microscopic Study. *J Neurovirol.* 2012;18: 503–10. [PMID: 23070817].
31. Prow TW, Raphael AP, Wurm EM, Longo C, Soyer HP. Cutaneous Photoaging: Description and Algorithms, In S. González (Ed.) Reflectance Confocal Microscopy of Cutaneous Tumors. CRC Press; 2017. [DOI: 10.1201/9781315113722].
32. Gill M, Longo C, Farnetani F, et al. Non-Invasive in Vivo Dermatopathology: Identification of Reflectance Confocal Microscopic Correlates to Specific Histological Features Seen in Melanocytic Neoplasms. *J Euro Acad Dermatol Venereol.* 2014;28: 1069–78. [PMID: 24147614].
33. Losi A, Longo C, Cesinaro MA, et al. Hyporeflective Pagetoid Cells: A New Clue for Amelanotic Melanoma Diagnosis by Reflectance Confocal Microscopy. *Br J Dermatol.* 2015;171: 48–54. [PMID: 24329036].
34. Nascimento MM, Shitara S, Enokihara MM, et al. Inner Gray Halo, a Novel Dermoscopic Feature for the Diagnosis of Pigmented Actinic Keratosis: Clues for the Differential Diagnosis with Lentigo Maligna. *J Am Acad Dermatol.* 2014;71: 708–15. [PMID: 24947988].